

airfoil ( $\Delta = \text{SPL}_{c,\text{thinnest}} - \text{SPL}_{c,\text{thicker}}$ ) increases linearly with frequency and also with increasing thickness.

The theoretical spectra at  $\theta_i = 90^\circ$  deg for a thin airfoil, which accounts for compressibility<sup>1</sup> are also shown in Fig. 2a as solid curves. According to the theory, frequencies to the right of the X on the curves are where compressible effects are important. The wiggles in the theoretical spectrum at very high frequency are due to the Fresnel integral term in the compressible theory.

The theory and data for the thin airfoil are in excellent agreement over the whole spectrum, including the wiggles. Only the absolute level of the set of theoretical spectra was adjusted for the best overall agreement to the data; all other inputs to the theory (summarized in Ref. 8) were as measured (i.e., transverse turbulence scale length,  $\ell_y$ ; peak impingement velocity,  $V_{ip}$ ; chord length, etc.).

In previous theoretical comparisons with thin airfoils,<sup>8</sup> the thinnest airfoil tested was 0.32 cm. The results shown in Fig. 2a indicate that the airfoil used in Ref. 8 was thin enough for thin airfoil theory to apply, except for very high frequencies. The thinnest airfoil tested in this experiment (0.082 cm) was impractically thin; indeed, special care was taken, and additional experiments were performed to insure that the thinnest airfoil data were not affected by vibration or deflection.

The effect of airfoil thickness upon the radiation patterns of the noise at three frequencies is shown in Fig. 2b for one velocity,  $V_{ip} = 94$  m/s. The highest and lowest frequencies were selected to avoid large jet noise corrections, while the middle frequency corresponds to the peak noise of the spectrum plotted in Fig. 2a.

The radiation patterns for the lowest and peak noise frequencies show no sizeable effect of thickness. On the other hand, the patterns for the highest frequency show a large effect of thickness; the thinnest airfoil is much noisier than the thick airfoil.

The theoretical pattern for a thin, small-chord airfoil in uniform turbulent flow ( $\sin^2\theta_i$ ) is put through the data at each frequency. The agreement is excellent at the low and peak frequencies, but the agreement is poor at high frequencies, even for the thinnest airfoil. This discrepancy with the thin airfoil data is probably due to the transverse velocity gradient across the airfoil thickness. There is no theory at this time to account for the effect of velocity gradients on the radiation pattern from a small airfoil. Existing theories that account for the effect of velocity gradients are for jet noise<sup>3</sup> and for edge noise from infinite plates.<sup>4</sup> These theories show that there is no effect of velocity gradients at  $\theta_i = 90^\circ$  deg; we took advantage of this fact in the spectral comparisons made in Fig. 2a.

The radiation pattern for the thick airfoil seems to curl up at large and small  $\theta_i$ , especially at high frequency. This effect is probably due to the "drag dipole," which was shown more clearly for thick airfoils in the data of Ref. 8. Fluctuating drag forces were neglected in the thin airfoil theory that produced the  $\sin^2\theta_i$  pattern.

Similar thickness-effect comparisons were also made (not shown) for the very large chord airfoils shown in Fig. 1. The agreement between the prediction from compressible-thin airfoil theory and the spectral data at  $90^\circ$  deg was again excellent. The effect of thickness on the spectra and radiation pattern was similar to that shown in Figs. 2a and 2b.

### Conclusions

This experiment expanded upon the thickness-effect aspect of the airfoil experiments performed in Ref. 8. The results show that the effect of thickness is large and must be accounted for in any fundamental airfoil noise theory that attempts to describe the noise emitted from real airfoils. Incident mean velocity gradients and compressibility must also be taken into account. The effect of thickness increases

with frequency, with thick airfoils being quieter than thin ones.

### References

- <sup>1</sup>Goldstein, M., *Aeroacoustics*, McGraw-Hill Book Co., New York, 1976, pp. 144, 137-145.
- <sup>2</sup>Goldstein, M. and Atassi, H., "A Complete Second-Order Theory for the Unsteady Flow About an Airfoil Due to a Periodic Gust," *Journal of Fluid Mechanics*, Vol. 74, April 1976, pp. 741-765.
- <sup>3</sup>Goldstein, M. and Howes, W., "New Aspects of Subsonic Aerodynamic Noise Theory," NASA TN D-7158, 1973.
- <sup>4</sup>Goldstein, M., "Scattering and Distortion of the Unsteady Motion of Transversely Sheared Mean Flows," *Journal of Fluid Mechanics*, Vol. 91, April 1979, pp. 601-632.
- <sup>5</sup>Olsen, W., Gutierrez, O., and Dorsch, R., "The Effect of Nozzle Inlet Shape, Lip Thickness, and Exit Shape and Size on Subsonic Jet Noise," AIAA Paper 73-187, Jan. 1973.
- <sup>6</sup>Olsen, W. and Friedman, R., "Jet Noise from Co-Axial Nozzles Over a Wide Range of Geometric and Flow Parameters," AIAA Paper 74-43, Jan. 1974.
- <sup>7</sup>Olsen, W. and Boldman, D., "Trailing Edge Noise Data with Comparison to Theory," AIAA Paper 79-1524, July 1979.
- <sup>8</sup>Olsen, W., "Noise Generated by Impingement of a Turbulent Flow on Airfoils of Varied Chord, Cylinders, and Other Flow Obstructions," AIAA Paper 76-504, July 1976.

AIAA 82-4069

## Active Attenuation of Acoustic Disturbances in Pulsed, Flowing Gas Lasers

M. J. Lavan\*

Ballistic Missile Defense Advanced Technology Center  
Huntsville, Ala.

and

F. W. French†

W. J. Schafer Associates, Wakefield, Mass.

### Introduction

IN pulsed, flowing gas lasers, only a small fraction of the pump energy is converted to laser output. Most of the energy goes into heat and acoustic waves which, until they eventually die out, distort the optical medium unacceptably. The laser pulse rate, which is limited by the acoustic relaxation time, can be increased by employing sidewall mufflers to speed up the damping process. In  $\text{CO}_2$  lasers, the required attenuation can be achieved with reasonable muffler volumes.<sup>1</sup> However, the order of magnitude more stringent density homogeneity needed for excimer lasers necessitates that very large, costly mufflers be used to meet the required 40 dB attenuation in sound power.<sup>2</sup>

For typical cavity dimensions of 0.50-1 m in the flow direction, most of the acoustic power is concentrated in the frequencies below a few hundred hertz.<sup>3</sup>

The effects of the lowest-frequency disturbances can be eliminated by fixed optical corrections.<sup>4</sup> The muffler volume is then driven by the need to attenuate the frequencies from a few ten to a few hundred hertz, which is the range over which active attenuation has been demonstrated.

The application of active attenuation<sup>5</sup> to the control of sound in laser ducts is best understood by an eigenmode<sup>6</sup>

Received May 14, 1981; revision received Aug. 31, 1981. This paper is declared a work of the U. S. Government and therefore is in the public domain.

\*Optics Directorate.

†Site Manager. Associate Fellow AIAA

analysis, because typical experimental data show that about 90% of the acoustic energy generated by the pump pulse is concentrated in the plane wave mode.<sup>7</sup> Swinbanks<sup>8</sup> showed that four monopole sources placed in the walls of a duct will generate only the plane wave mode for any frequency up to the "cut-on" frequency of the (2,2) mode, which is a few hundred hertz for a laser duct.

Active attenuators have been demonstrated in ducts with average noise attenuation as much as 15 dB over the 31.5-200 Hz interval.<sup>9,10</sup> The single-frequency attenuations of up to 50 dB also obtained could be useful as a means of suppressing the standing waves that can build up in lasers.<sup>11</sup>

### Application of Active Acoustics to Pulsed Lasers

A conceptual design for the application of an active attenuator to lasers is shown in Fig. 1. Acoustic waves propagate out of the optical cavity and are reflected back toward the cavity by the thermal interface of the previous pulse. The attenuator sources would be located just downstream of the cavity, with the system's detectors slightly further downstream. Sequential detectors would resolve the direction of propagation to insure that the system attempts to attenuate only the weak, residual waves that have been reflected from the thermal interface and have thus undergone two passages through the section of duct containing the passive attenuator.

In order to quantify the potential benefits of active attenuation, we have calculated the muffler volumes required for a 40 dB reduction in laser sound power with active attenuators in a system and compared it to the muffler volume required without active attenuators. The laser cavity was taken to be 0.5 m in the flow direction, with a duct cross section of  $0.5 \times 2.0$  m and a gas sound speed of 550 m/s.

The sidewall muffler model used is a series of Helmholtz resonators, each of a different volume and resonant frequency, as shown schematically in Fig. 1. The total attenuation of the acoustic wave is given by the ratio of  $P_{in}$ , the acoustic power re-entering the optical cavity to  $P_{out}$ , the acoustic power radiated out of the cavity. Thus,

$$\frac{P_{in}}{P_{out}} = \frac{\int_{f_m}^{f_M} P^2(f) A^2(f) K(f) df}{\int_{f_m}^{f_M} P^2(f) df} \quad (1)$$

The acoustic power spectral density,  $P^2(f)$ , of the pressure waves radiating out of an optical cavity of length  $L$  is well approximated by the Fourier transform of a square wave,<sup>12</sup> so

$$P^2(f) \propto \text{sinc}^2(\pi L f / C) \quad (2)$$

where  $C$  is the speed of sound. As the pressure wave propagates past the sidewall muffler in either direction, it undergoes an attenuation  $A(f)$  given by  $A_1(f), A_2(f), \dots, A_N(f)$ , the product of the individual resonator attenuations, where  $A_K(f)$  is given by<sup>3</sup>

$$A_K(f) = \left[ 1 + \frac{\alpha + 0.25}{\alpha^2 + \beta^2 (f/f_K - f_K/f)^2} \right]^{-1} \quad (3)$$

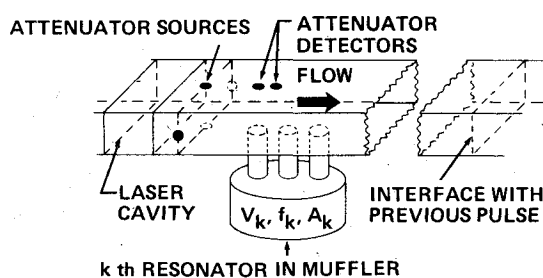


Fig. 1 Schematic of combined attenuation system.

The parameters  $\alpha$ ,  $\beta$ , and  $f_K$  are determined by the laser gas and the characteristics of the resonator and duct.<sup>3</sup> The final factor  $K(f)$  in the integral represents the effects of the active attenuator. For the baseline case, when active attenuation is not considered,  $K(f)$  is identically equal to one for all frequencies. The presence of an active attenuator is modeled by evaluating the integral with  $K(f)$  equal to some constant  $K$  over a given range of frequencies.

The upper limit of the integral,  $f_M$ , is taken to be sufficiently great (15.2 kHz) that the numerical integral over the power spectral density function is at least 99% of its theoretical value. The selected lower limit,  $f_m$  (25 Hz), satisfies the requirement that the corresponding acoustic wavelength be many multiples of the optical cavity in length. For a given laser cavity length, gas mixture, and duct area, we first fix  $\alpha$  and  $\beta$  at reasonable values,<sup>3</sup> and then pick a distribution of 25-30 resonant frequencies. This fixes the volumes of the individual resonators, and thus the total muffler volume. By a trial and error variation of  $\alpha$ ,  $\beta$ , and the resonant frequencies, the muffler volume needed to achieve the required 40 dB attenuation is then minimized for a given active attenuator.

### Results and Discussion

The solid curves of Fig. 2 show the combined active attenuator/passive muffler combinations needed to achieve an attenuation of 40 dB. The curves are labeled by the range of frequencies actively attenuated. A fourth curve, showing the performance of a system operating from 25 to 500 Hz, differs only negligibly from the curve shown for the 25-250 Hz system. The insignificant further improvement follows because of the fall-off in acoustic power at the higher frequencies, and because of the effective attenuation provided by the passive mufflers at those frequencies. Therefore, as expected, the biggest payoffs come from improving performance at the low frequencies; however, very narrow active attenuation performance bands do not lead to great reductions in the muffler volume, regardless of how strong an attenuation is provided. Thus, the muffler volume reduction for the active attenuator operating from 25 to 75 Hz is limited to about 10%, because much of the acoustic flux lies in the frequencies between 75 and 125 Hz, a band which requires a rather bulky muffler.

The acoustic source performance characteristics required to implement an active attenuator can be readily estimated for a 1 kW excimer laser pumped by a 20 kW electron-beam pump. Typically, 40% of the pump power would be converted to acoustic waves. However, only about 0.2% of the acoustic energy will be reflected by the thermal interface back toward the optical cavity,<sup>2</sup> so the power to be attenuated is just 16 W.

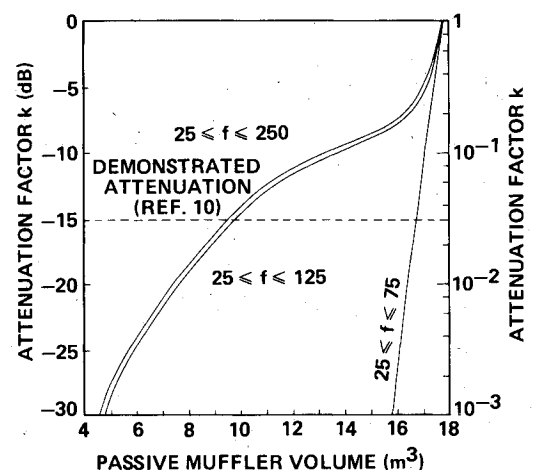


Fig. 2 Performance of active attenuator passive muffler combinations.

The performance curves in Fig. 2 show that the combination of an 11.3 m<sup>3</sup> sidewall muffler and an active attenuator operating in the 25-125 Hz band will provide the required attenuation. Detailed calculations show that about 20% of the acoustic energy to be attenuated lies in the 25-125 Hz band; and the round-trip passage through the sidewall muffler attenuates that band by a factor of 0.007 to 0.022 W.

Thus, an active attenuator emitting only a few hundredths of a watt would enable a reduction in the passive muffler volume of about 35%. Since even a simple piston speaker can achieve 4% efficiency for narrow frequency ranges, only about 1 W of power would be required to drive the four speakers. If the laser were operated at a few atmospheres pressure, the characteristic acoustic impedance of the laser gas would increase, with a corresponding improvement in speaker efficiency. Another possibility for improving speaker efficiency would be to use an acoustic horn, providing its presence did not cause an unacceptable perturbation in the gas flow.

### References

- Feinberg, R., Lowder, R. S., and Zappa, O., "Low Pressure-Loss Cavity for Repetitively Pulsed Electric Discharge Lasers," AFWL-TR-75-99, 1975.
- Hogge, H. D. and Crow, S. C., "Flow and Acoustics in Pulsed Excimer Lasers," AIAA Paper II-4, Nov. 1978.
- Embleton, T. F. W., "Mufflers," *Noise and Vibration Control*, 1st ed., McGraw-Hill, New York, 1971, pp. 362-405.
- Srivastava, B. N., Knight, C. J., and Zappa, O., "Acoustic Suppression in a Pulsed Laser System," AIAA Paper 79-0209, Jan. 1979.
- Lueg, P., "Process of Silencing Sound Oscillations," U. S. Patent No. 2043416, 1936.
- Morse, P. M. and Ingard, K. U., *Theoretical Acoustics*, 1st ed., McGraw-Hill, New York, 1968, pp. 467-607.
- Daugherty, J. D., AVCO Everett Research Laboratories, private communication.
- Swinbanks, M. A., "The Active Control of Sound Propagation in Long Ducts," *Journal of Sound and Vibration*, Vol. 27, No. 3, 1973, pp. 411-436.
- Poole, J. H. B. and Leventhall, H. G., "An Experimental Study of Swinbanks' Method of Active Attenuation of Sound in Ducts," *Journal of Sound and Vibration*, Vol. 49, No. 2, 1976, pp. 257-266.
- Poole, J. H. B. and Leventhall, H. G., "Active Attenuation of Noise in Ducts," *Journal of Sound and Vibration*, Vol. 57, No. 2, 1978, pp. 308-309.
- Tong, K. O. et al., "Flow and Acoustics Study for Pulsed Visible Lasers," AIAA Paper, 80-0348, Jan. 1980.
- Cason, C., Karr, G. R., and Shih, C. C., "Structure and Propagation of Waves Generated in a Pulsed High Energy Gas Laser," *Gas-Flow and Chemical Lasers*, 1st ed., Hemisphere, Washington, 1979, pp. 285-295.

AIAA 82-4070

## Correction of Stiffness Matrix Using Vibration Tests

Menahem Baruch\*

Technion—Israel Institute of Technology,  
Haifa, Israel

IN a recent Note<sup>1</sup> Wei reobtains the corrected stiffness matrix given in Refs. 2-5. It is interesting that, by algebraic manipulations, Wei succeeds in eliminating the Lagrange multiplier  $\lambda_y$  from the derivation. In this way the need to calculate  $\lambda_y$  is avoided. Unger and Zalmanovich<sup>6</sup> proposed

different constraints from those used in Ref. 3. These constraints constitute of the requirement that the corrected measured modes must be orthogonal between themselves and in addition must also be orthogonal to the unmeasured modes. In this way, Zalmanovich<sup>7</sup> succeeds in obtaining the necessary Lagrange multipliers and the corrected stiffness matrix without any additional assumptions.

In Ref. 3 the Lagrange multiplier  $\lambda_y$  was obtained by making the assumption that the matrix  $\lambda_y' M X$  is symmetric. In his Note,<sup>1</sup> Wei makes the remark that this assumption "is not always true in general and is hard to understand from a physical point of view." In what follows, the meaning of the assumption is given and it is shown that it is a permissible assumption and therefore true.

The corrected stiffness matrix  $Y$  was obtained in Refs. 2-5 by minimization of the weighted Euclidean norm

$$g = \frac{1}{2} \|N^{-1} (Y - K) N^{-1}\| \quad (1)$$

where

$$N = M^{1/2} \quad (2)$$

$M$  is the mass matrix,  $Y$  ( $n \times n$ ) the corrected stiffness matrix, and  $K$  ( $n \times n$ ) a given stiffness matrix.

The corrected stiffness matrix  $Y$  must satisfy the following constraints<sup>2-5</sup>

$$YX = MX\Omega^2 \quad (3)$$

and

$$Y = Y' \quad (4)$$

where  $\Omega^2$  ( $m \times m$ ) represents the measured frequencies and  $X$  ( $n \times m$ ) the already orthogonalized incomplete set of measured modes<sup>2-5</sup>

$$X' M X = I \quad (5)$$

The constraints of Eqs. (3) and (4) were incorporated in Eq. (1) by using Lagrange multipliers. Minimization of the cost function  $g$ , with respect to  $y_{ij}$  and elimination of the Lagrange multiplier connected with Eq. (4) gave<sup>2-5</sup>

$$Y = K - M\lambda_y X' M - M X \lambda_y' M \quad (6)$$

where  $\lambda_y$  ( $n \times m$ ) is the Lagrange multiplier connected with the constraint of Eq. (3). Using this last constraint the following equation was obtained

$$M X \Omega^2 = K X - M\lambda_y - M X \lambda_y' M X \quad (7)$$

Here the following crucial assumption was made

$$\lambda_y' M X = X' M \lambda_y \quad (8)$$

The assumption of Eq. (8) was used in Ref. 3 to obtain the corrected stiffness matrix [Ref. 3, Eq. (23)]

$$Y = K - K X X' M - M X X' K + M X X' K X X' M + M X \Omega^2 X' M \quad (9)$$

In Ref. 3 it was shown that although  $\lambda_y$ , which satisfies Eq. (7) is not unique, the corrected stiffness matrix obtained from any such  $\lambda_y$  is the same and is given in Eq. (9). In other words, any assumption for  $\lambda_y$  that does not violate Eqs. (3), (7) and itself is true and can be used to obtain  $Y$ . More than that, Eq. (8) has also a clear physical and mathematical meaning.

In the minimization process in Ref. 3 the constraint of Eq. (3) was taken formally to represent  $mn$  independent constraints. However, due to the fact that the mode shapes  $X$  are orthogonal, one obtains

$$X_i' Y X_j = 0 \quad i \neq j \quad (10)$$

Received July 6, 1981. Copyright © American Institute of Aeronautics and Astronautics, Inc., 1981. All rights reserved.

\*Professor, Department of Aeronautical Engineering. Member AIAA.